ELSEVIER

Nuclear Instruments and Methods in Physics Research A 424 (1999) 84–91

NUCLEAR INSTRUMENTS & METHODS IN PHYSICS RESEARCH Section A

An 800-MeV proton radiography facility for dynamic experiments

N.S.P. King[a,*], E. Ables[b], Ken Adams[a], K.R. Alrick[a], J.F. Amann[a], Stephen Balzar[c], P.D. Barnes Jr.[b], M.L. Crow[a], S.B. Cushing[a], J.C. Eddleman[a], T.T. Fife[a], Paul Flores[c], D. Fujino[b], R.A. Gallegos[a], N.T. Gray[a], E.P. Hartouni[b], G.E. Hogan[a], V.H. Holmes[a], S.A. Jaramillo[a], J.N. Knudsson[a], R.K. London[a], R.R. Lopez[a], T.E. McDonald[a], J.B. McClelland[a], F.E. Merrill[a], K.B. Morley[a], C.L. Morris[a], F.J. Naivar[a], E.L. Parker[b], H.S. Park[b], P.D. Pazuchanics[a], C. Pillai[a], C.M. Riedel[a], J.S. Sarracino[a], F.E. Shelley Jr.[a], H.L. Stacy[a], B.E. Takala[a], Richard Thompson[c], H.E. Tucker[a], G.J. Yates[a], H.-J. Ziock[a], J.D. Zumbro[a]

[a] *Los Alamos National Laboratory, Los Alamos, NM 87545, USA*
[b] *Livermore National Laboratory, Livermore, CA 94550, USA*
[c] *Bechtel Nevada, Los Alamos, NM 87545, USA*

Abstract

The capability has successfully been developed at the Los Alamos Nuclear Science Center (LANSCE) to utilize a spatially and temporally prepared 800 MeV proton beam to produce proton radiographs. A series of proton bursts are transmitted through a dynamic object and transported, via a unique magnetic lens system, to an image plane. The magnetic lens system permits correcting for the effects of multiple coulomb scattering which would otherwise completely blur the spatially transmitted information at the image plane. The proton radiographs are recorded either on a time integrating film plate or with a recently developed multi-frame electronic imaging camera system. The latter technique permits obtaining a time dependent series of proton radiographs with time intervals (modulo 358 ns) up to many microseconds and variable time intervals between images. One electronically shuttered, intensified, CCD camera is required per image. These cameras can detect single protons interacting with a scintillating fiber optic array in the image plane but also have a dynamic range which permits recording radiographs with better than 5% statistics for observation of detailed density variations in the object. A number of tests have been carried out to characterize the quality of the proton radiography system for absolute mass determination, resolution, and dynamic range. Initial dynamic experiments characterized the temporal and spatial behavior of shock propagation in a high explosive sample with up to six images per experiment. Based on experience with the prototype system, a number of upgrades are being implemented including the anticipated capability for enhanced mass discrimination through differential multiple coulomb scattering radiographs and more images with improved imaging techniques.

* Corresponding author. Tel.: + 1 505 667 6306; fax: + 1 505 665 4121; e-mail: nspk@lanl.gov.

0168-9002/99/$ – see front matter
PII: S0168-9002(98)01241-8

1. Introduction

Classical radiography typically involves uncharged incident radiation such as X-rays or neutrons, a portion of which is transmitted through an object of interest to a detector plane forming a shadow-graph. Important features of these systems which affect the quality of the resultant projected image onto the detector plane include source size, incident and transmitted flux, detector blur, scattered backgrounds, and detector efficiency. The utility of these radiographs to view various aspects of the object is closely related to the integrated mean free path for removal of the incident radiation and the interaction of the transmitted flux with the detector. A background from scattering from surrounding material as well as from different parts of the object results in reduced contrast. Spatial resolution can be strongly affected by the size of the source as well as the statistics associated with detecting the transmitted radiation. The issue of image statistics is compounded by the fact that both neutrons and X-rays are secondary products of primary charged particle production techniques. This necessarily results in lower incident fluxes on objects to be radiographed than would be possible using charged particles directly. Problems with low detector efficiencies are frequently encountered due the necessity of reconverting incident radiation to charged particle channels. The highly localized energy deposition resulting from the large interaction cross sections for thermal neutrons are an exception.

Obtaining high quality proton radiographs depends upon related but also different issues than for neutral radiation. The fundamental processes for interaction of the incident proton flux are nuclear processes for attenuation, multiple Coulomb scattering (MCS), and energy loss. The latter processes result in additional complexity in forming a radiograph but can also provide unique possibilities for increased sensitivity to material features in the object. The development and use of magnetic lenses is necessary to compensate for the small angle MCS which in effect destroys the transmitted "image" through an object. The mean MCS angle is inversely proportional to the incident proton momentum and proportional to the square root of the object thickness. The practical application of proton radiography is therefore a tradeoff between incident momentum and object thickness since the angular acceptance of a lens may become impractical large for low momentum protons and thick objects. A schematic of a proton radiographic system is presented in Fig. 1. The image plane detector for our system is either an in-beam film plate or a scintillator with few nanosecond decay time which is lens coupled to electronic cameras. The 800 MeV proton system at LANSCE is currently optimized for radiographing objects with integrated areal densities near 50 g/cm^2. It should be mentioned however that much thicker objects can in fact be radiographed but will require increased numbers of protons for good statistics to compensate for losses due to specific magnetic lens apertures. These numbers can in fact be obtained by increasing the

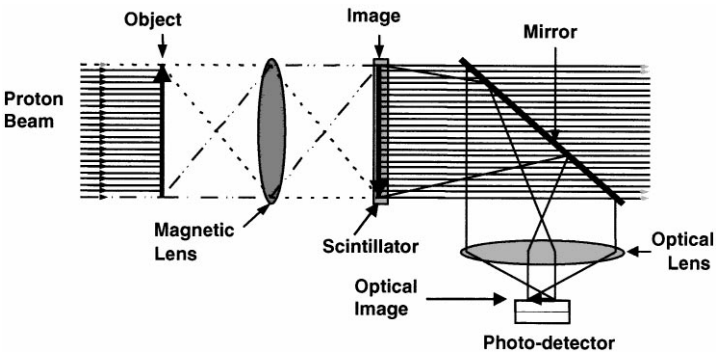

Fig. 1. Schematic of proton radiography system.

proton burst width at a sacrifice in temporal resolution for dynamic experiments. For static radiographs this is not a limitation in any case. An energy selective detector in the image plane can take advantage of differential energy loss for material selection for different regions of an object. A number of such detector options are possible such as those based on Cherenkov processes but will not be discussed further. The following sections describe current experience with proton radiography at 800 MeV as well as relevant concepts and limitations.

2. Proton interaction processes

The processes important to proton radiography are summarized in Fig. 2. Transmission radiography results from an exponential attenuation of the incident proton flux by nuclear processes contributing to the mean free path for removal of a proton from the detection system. This can include the fraction of nuclear elastic scattering not collected by the magnetic lens system. Coulomb multiple scattering at large angles can also effectively remove a fraction of the transmitted protons from the image plane. This feature can provide a unique capability for proton radiography. The detector in the initial image plane can be constructed to permit further transport of the "image" protons through a second magnetic lens system which has a smaller angular acceptance which then preferentially removes protons having the largest MCS angles in a second image plane. These image regions will correspond to those object areas containing more dense or possibly higher Z materials. It should be mentioned that the detector systems for protons can be made highly efficient in that charged particle detection is dependent upon Coulomb interactions rather than through the formation of secondary charged particles as in the case of X-rays or neutrons. This results in the potential for making images with very high statistics for a relatively small number of transmitted particles since each proton can in principle be detected.

TRANSMISSION

$$\frac{N_1}{N_0} = e^{-\sum \frac{l_i}{\lambda_i}}$$

so,

$$\sum \frac{l_i}{\lambda_i} = -\ln\left(\frac{N_1}{N_0}\right)$$

MULTIPLE SCATTERING

$$\frac{N_2}{N_1} = \frac{1}{2\pi\theta_0^2}\int_0^{\theta_m} e^{-\frac{\theta^2}{2\theta_0^2}} d\Omega \cong \left[1 - e^{-\frac{\theta_m^2}{2\theta_0^2}}\right]$$

where,

$$\theta_0 \approx \frac{14.1}{p\beta}\sqrt{\sum \frac{l_i}{L_{Ri}}}$$

so,

$$\sum \frac{l_i}{L_{Ri}} = -\frac{(p\beta\theta_m)^2}{2(14.1)^2 \ln\left(1 - \frac{N_2}{N_1}\right)}$$

Fig. 2. Mathematical summary of proton radiography processes.

3. Magnetic lens and proton beam properties

The magnetic lens system utilized in 800 MeV proton radiography at LANSCE is shown in Fig. 3. A diffuse beam is generated over the object plane by introducing adjustable thickness stainless steel (≤ 1.5 mm) at a location upstream from a quadrupole magnet pair. This results in a divergent beam in the horizontal plane and convergent beam in the vertical plane with a specific correlation between positions and angle at the object location.

The protons transmitted through the object are transported by the "lens" system consisting of four matched quadrupoles to the image plane with a magnification minus one. This condition is chosen to minimize chromatic aberrations and results in uniform acceptance over the field of view. The entire magnetic lens system can be approximated by simple ray tracing of "optical" rays much like a pinhole or simple lens located at the center of the lens. More details can be found in Ref. [1]. The depth of field for this system can be estimated from the angular acceptance of such a simple lens geometry and results in about a ± 25 mrad correlation angle in the image plane for the horizontal (vertical) plane at the edge of the field of view. This results in a projected resolution of about 2 lp/mm for the extreme rays at the edge of the field of view for an image plane depth of 2 cm. This scales to about 4 lp/mm for a central field of view of 6.4 cm. Added to this resolution is the angular spread about each central ray trajectory due to the maximum MCS angle. This is limited by the collimator

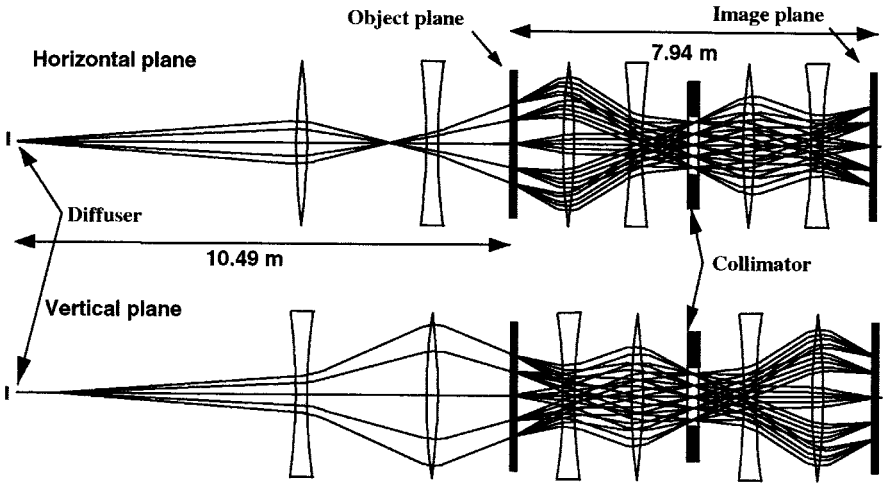

Fig. 3. X- and Y- plane ray traces for the magnetic lens system used in initial experiments. The incident proton beam was expanded with a diffuser and an upstream lens doublet, which also established a correlation between particle location and angle at the object plane. The correlation reduced aberrations in the subsequent inverting identity lens. The identity lens consisted of four quadrupole magnets. Multiple Coulomb scattering of the proton beam by the object is schematically indicated. Scattered rays are at angles of ± 10 and ± 5 mrad with respect to a 0 mrad on axis ray. The radial angle sorting at the mid-plane of the lens (collimator location) is clearly seen. (The transverse scale is greatly expanded to the longitudinal scale in which the magnetic aperture shown is 20 cm.)

at the center of the quadrupole pairs and is typically ± 10 mr as well. The final resolution is then a convolution of these effects. Optimization of the magnetic lenses is required due to energy loss for different objects.

A typical beam profile is a burst of 7 proton pulses (200 ps/pulse) each separated by 5 ns with bursts repeated at programmed intervals. The number of protons per pulse is typically 5×10^8. The beam area is contained within a 12×12 cm^2 field of view. The capability of generating a series of proton bursts, each containing a programmable number of micro-pulses permits varying both the "exposure" time per image as well as the option of multiple images at different times. The imaging detector system utilizing electronic cameras can be shuttered to isolate different images corresponding to different proton bursts. The radiation to light converter time "blurs" the pulses separated by 5 ns into a continuous light burst at the detector. The film plates give a "time integrated" image. A typical 50 ns burst pattern can be repeated as frequently as 358 ns. Longer separations with non-uniform spacing are possible modulo 358 ns. The 358 ns minimum time separation between bursts and the multiplying factor for multiple bursts is a current feature of our accelerator pulse programmer and not a fundamental limitation of the LANSCE accelerator system.

4. Image plane detectors

Image plane detector system requirements are dictated by a desire to exceed the resolution obtainable from the other radiographic system components such as the magnetic lens. The object plane field of view has a diameter of 127 mm and is equal to that in the image plane for a magnetic lens magnification of -1.0. The detailed, non-image plane resolution performance is complicated in that it depends to some extent on energy loss effects which are object specific and the requirements for entrance and exit windows in a containment system for high explosive (HE) experiments. Data obtained with a large format, phosphor image plate system with a resolution close to 10 lp/mm permits evaluating resolution effects for a number of simple

objects. These static images are not limited by statistics associated with the number of transmitted protons. The image plates have an efficiency of about 50% per proton. The response of the image plate system to varying radiation intensity was evaluated with a radioactive source. No corrections were found necessary to permit obtaining quantitative radiographic density variations better than 5%. An example of a single image plate radiograph is shown in Fig. 4. The resolution object is a 2 mm thick platinum "comb" in which the finest grooves are 0.5 mm. The system resolution is clearly much better than this. The "onion skin" explosive mockup is a graphite hemisphere with a 0.25 mm aluminum shell imbedded in it to simulate a 30% higher density high explosive "burn front". Initial dynamic experiments involved explosive assemblies similar to this which were placed in a 122 cm diameter steel, containment vessel with entrance and exit pipes for the proton beam. The entrance pipe had a 1.27 cm thick aluminum entrance window and the exit pipe extended through the lens system to a 1.27 cm exit window within 1 cm of the image plane. Image plates were mounted to the exit window for static or single image radiographs. For electronic imaging a 2.5 cm thick scintillating fiber array was placed at the exit window. This array was made from 300 μm core, circular fibers with a time response of about 3.5 ns. As shown in Fig. 5, the light from the array was reflected into multiple, gated, intensified, cooled CCD cameras. The number of protons per experiment was low enough that radiation shielding of the camera system was not needed. All cooled, CCD cameras were fiber optically coupled to their respective gated intensifiers. Different gated intensifier, CCD camera combinations were utilized with Nikon 105 mm f1.8 or 135 mm f2.0 lenses. The intensifiers served the purpose of providing necessary optical shuttering and wavelength shifting from the 415 nm scintillator light to a P43 phosphor light which has a high quantum efficiency for detection by the CCD arrays. Proven 200 V gating techniques with microchannel plate image intensfiers (MCPII) were used

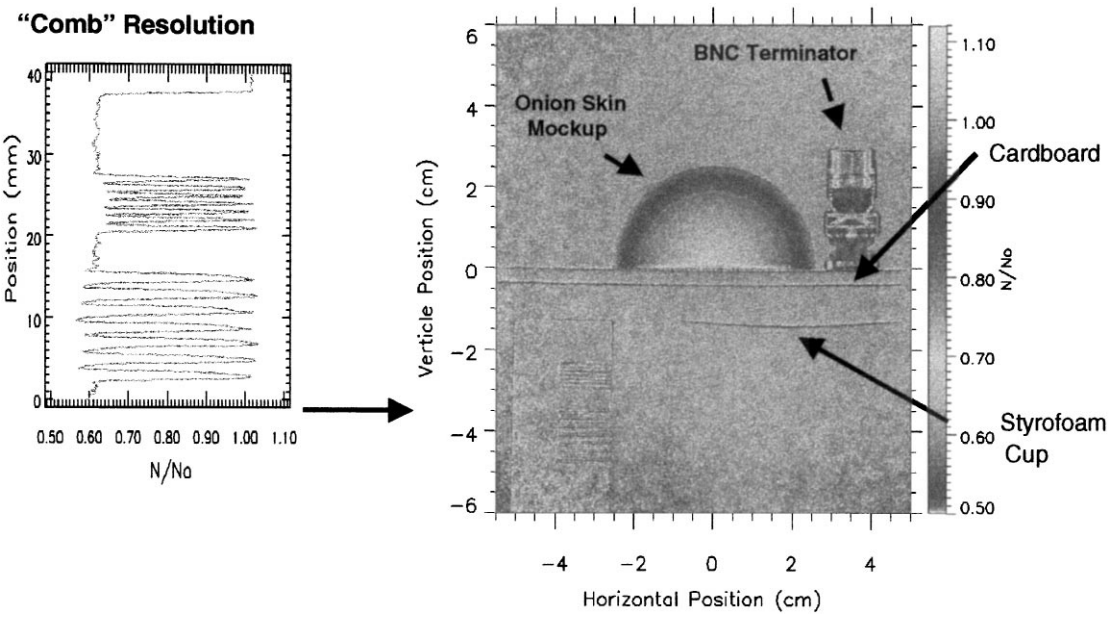

Fig. 4. Images for test objects taken with a single image plate. Objects are a platinum "comb", a graphite hemisphere with imbedded aluminum shell, and a 50 Ω terminator. The latter two objects are mounted on a cardboard support placed on an inverted styrofoam drinking cup.

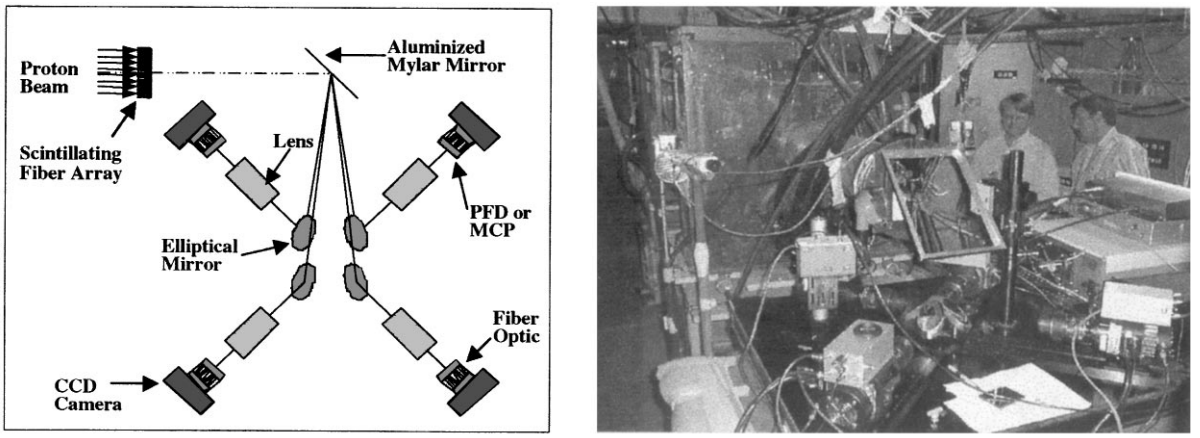

Fig. 5. Schematic of the imaging detector system for proton radiography experiments is shown on the left. A photograph of the system is shown on the right. The cameras and lenses shared a common horizontal mounting plate located 46 cm below the proton beam.

as well as new 10 KV gates on planar diodes. Typical optical shutter times were 350 ns. Transmitted fluxes of 10^5 protons/mm^2 in the image plane for a 50 ns burst resulted in 60% full pixel well signals for the planar diode gated, 1024×1024, CCD pixel arrays. Very low gains were required in the MCPII based systems to avoid saturation of their 512×512 pixel CCD arrays. As a consequence, the MCPII based systems had poorer signal to noise characteristics compared to the planar diode based cameras. This is the result of a loss in photoelectrons due to the MCP prior to the P43 phosphor screens. Based on a statistical analysis of a series of images, a detection quantum efficiency (DQE) of 0.6 and 0.4 were obtained for the planar diode/1024pixel and MCPII/512pixel camera systems. This can be related to the number of detected photoelectrons per proton being 1.5 and 0.66, respectively. A dynamic range of $\geq 10^4 : 1$ has been measured for the camera systems. More details on the electronic system are given in Ref. [2].

5. Dynamic results

An example of three images from three gated cameras is shown in Fig. 6. The first column corresponds to the ratio between static images taken with and without the object present under the same proton beam conditions. The second column is a ratio between a series of dynamic images taken at the times noted and the same image used in the first column without the object present. Shutter widths were 350 ns as mentioned previously with a proton burst width of 50 ns. The last column is a ratio between the dynamic sequence and the corresponding camera static images with the object present. A series of five static images with the object present were recorded just prior to igniting the high explosive to permit obtaining an average static image for analysis. This gave a better signal to noise in the ratio of dynamic to static images. One can clearly see the evolution of the high explosive burn front from the top to bottom images in the dynamic images.

A second series of images taken with film plates in four separate experiments is shown in Fig. 7. The first column is a ratio of static to dynamic data and is similar to the third column in the previous figure. A reconstruction algorithm assuming cylindrical symmetry has been used to obtain density slices from the experimental areal densities. These slices clearly show the desired temporal behavior in the "burn front" density variations needed to provide quantitative information for improving high explosive models.

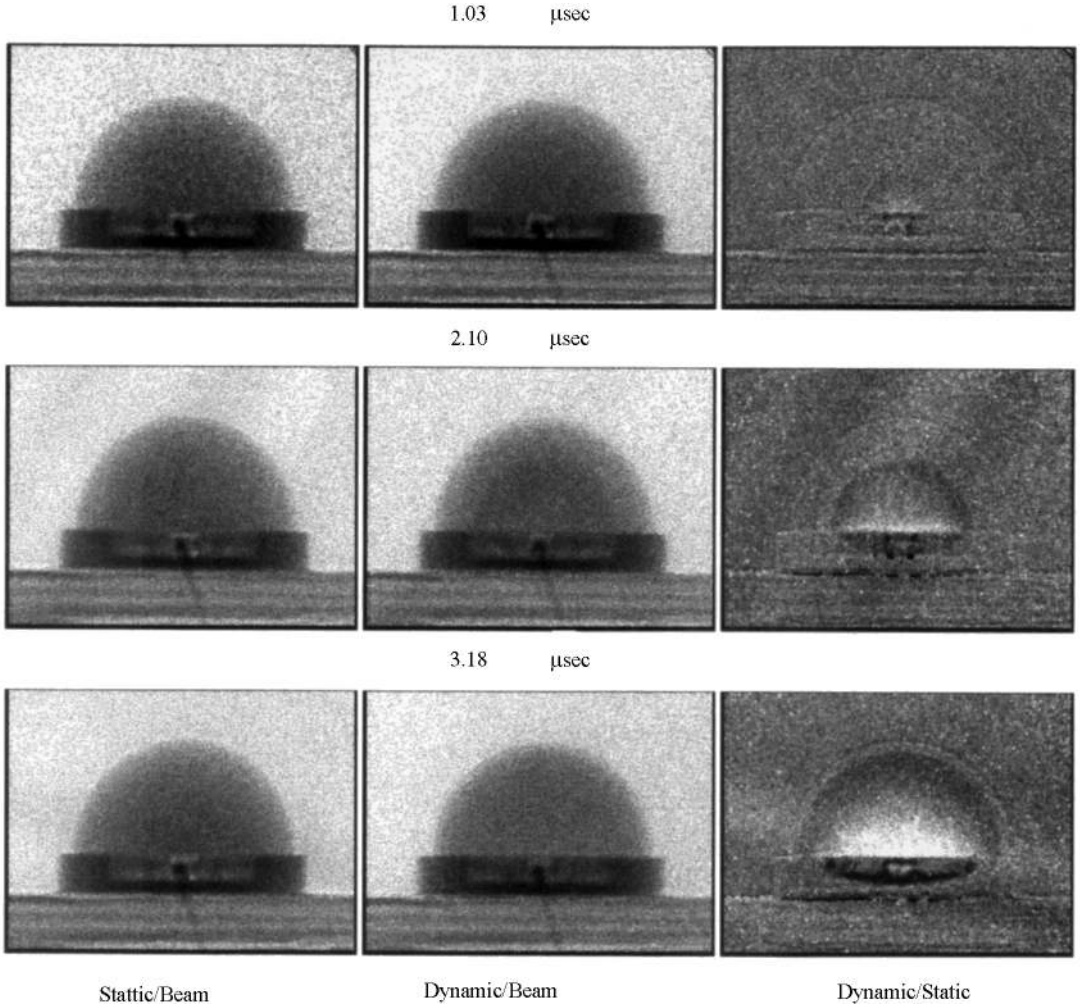

Fig. 6. Three sequential electronic images for a hemispherical, high explosive experiment.

6. Conclusions

A series of static and dynamic experiments have been performed to demonstrate the capability of utilizing 800 MeV protons to obtain radiographs of high quality. Unique features of high statistics, high detection efficiency, and multiple pulses with a high resolution magnetic lens provide a powerful, quantitative tool for radiographic experiments. Resolution of $\leq 200\,\mu m$ has been achieved with time response ≤ 50 ns with up to 6 multiple images in dynamic experiments.

The current system for 800 MeV radiography is an upgrade to the system used in the initial experiments described above in that it contains a multiple lens system to vary the accepted multiple scattering angle for enhanced material identification in two image planes. Different collimator sizes will permit obtaining two radiographs per proton pulse in two image planes. The incident beam profile can also be captured on a pulse by pulse basis for normalization purposes. Seven individual cameras per image plane based on gated planar diodes provide the electronic images.

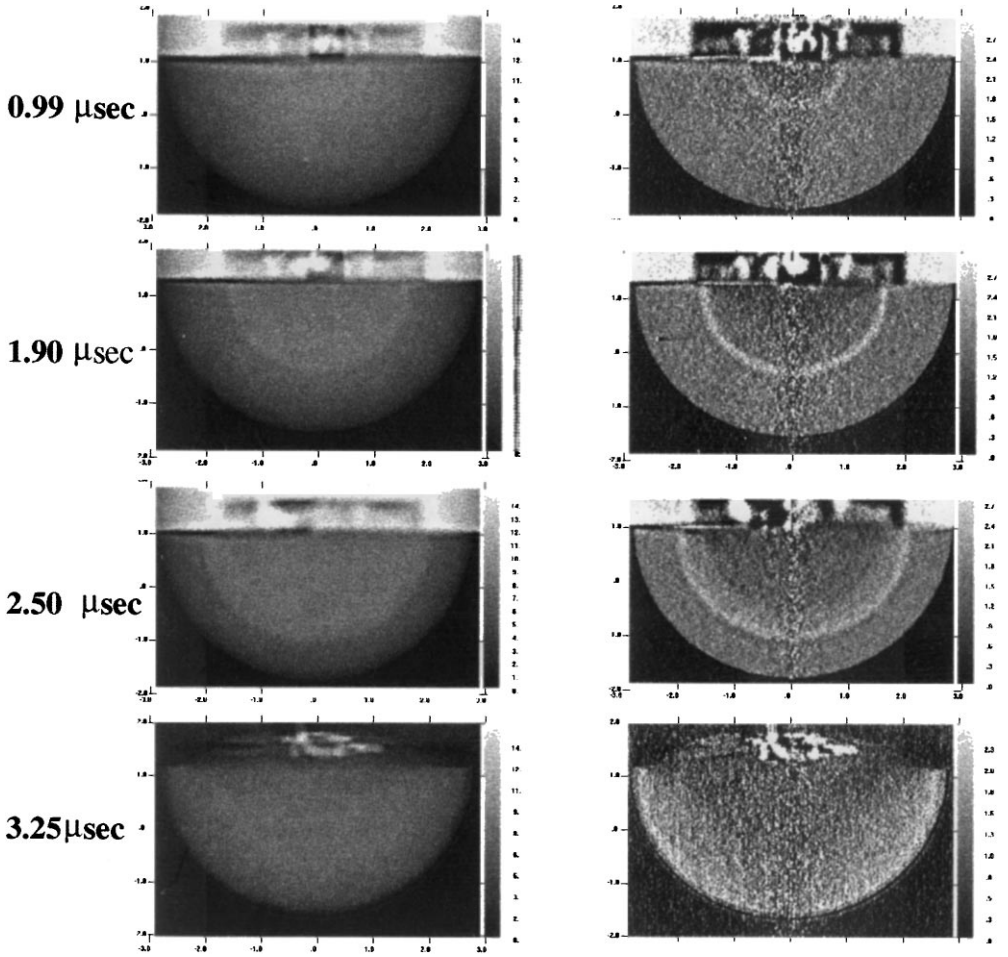

Fig. 7. Dynamic image ratio with average static image (left) and reconstructed images assuming cylindrical symmetry to permit obtaining volume density distributions as a function of time (right).

It is anticipated that the magnetic lens can be operated to provide a magnification of 3 : 1 for enhanced resolution requirements with a single image plane. This will result in a reduced object field of view.

References

[1] C.T. Mottershead, J.D. Zumbro, in: Proc. Particle Accelerator Conf., Vancouver, Canada, May 1997.
[2] G.J. Yates et al., in: Proc. Electronic Imaging '98 Conf. San Jose, CA, 24–30 January 1998.